Grenze International Journal of Engineering and Technology, June Issue

Synthesis of Dysprosium Molybdate as an Electrocatalyst for the Detection of Chloramphenicol

Sahana K M[1], Varun D N[2], Sandeep S[3] and Santhosh A S[4]
[1]Department of Chemistry, SJCE, JSS Science and Technology University, Mysuru, Karnataka, India.
[2-4]Department of Chemistry (UG), NMKRV College for Women, Jayanagar 3rd block, Bengaluru, Karnataka, India.
Email: sandeep12chem@gmail.com

***Abstract*—In this work, Dysprosium Molybdate (DyM) nanoparticles were synthesised using a simple co-precipitation method and evaluated for their potential as an electrochemical sensor for the detection of Chloramphenicol (CAP), a widely used but highly toxic antibiotic. The synthesised DyM was characterised by XRD and HRTEM, confirming its crystalline monoclinic phase and nanoscale morphology. The DyM was fabricated onto a pencil graphite electrode (PGE) and tested using electrochemical techniques including Cyclic Voltammetry (CV), electrochemical Impedance Spectroscopy (EIS), and differential pulse voltammetry (DPV). The modified PGE/DyM electrode exhibited remarkable electrocatalytic activity towards CAP, achieving a low limit of detection (0.7488 µM), high sensitivity (18.87 µA mM-1 cm-2), and a linear response range of 100-1000 µM. the sensor also demonstrated good stability, repeatability, and reproducibility, highlighting its suitability for practical CAP monitoring in environmental and pharmaceutical samples.**

I. INTRODUCTION

The use of antibiotics is prevalent in both animal and human medicine, attributed to their effectiveness in combating and preventing bacterial infections [1]. Chloramphenicol (CAP), illustrated in Fig.1 is a neutral derivative of nitrobenzene and is widely utilized as an antibiotic for the treatment of infections caused by both gram-positive and gram-negative bacteria [2]. Cap exhibits favourable pharmacokinetic characteristics; however, its side effects encompass bone marrow suppression, aplastic anemia, and gray baby syndrome. Due to its toxicity in humans, the use of CAP in food-producing animals has been entirely prohibited in the European Union.

Consequently, it is crucial to develop a cost-effective, straightforward, and sensitive detection method for CAP [4]. The primary methods for detecting antibiotic residues include chromatography, microbial assays, and electrochemical analysis. However, chromatographic techniques are limited to laboratory use because of their expensive equipment, high operational costs, complex experimental designs, transportation issues, and other related challenges [5]. Among the various methods available, the electrochemical approach is notable for its straightforwardness and affordability [6].

Over the last several decades, there has been significant research into metal oxide nanomaterials across a wide range of fields, with applications spanning electrochemical detection, solar energy conversion, supercapacitors, and photocatalytic processes [7]. The integration of hetero-metal oxides into a single metal oxide has proven to be an effective strategy for modifying grain size, phase structure, electrical conductivity, and band gap, thereby synergistically improving the sensing characteristics [8].

Grenze ID: 01.GIJET.11.2.764

Binary metal oxide nanostructures have recently attracted significant interest from researchers in various fields due to their beneficial characteristics, including semiconducting properties and synergistic coupling in metal-metal interactions. Among the periodic metals, the rare earth (RE) lanthanides-such as LA, CE, Pr, Nd, Pm, Sm, Eu, Gd, Tb, Dy, Ho, Er, Tm, and Yb-are well recognized for their outstanding optical, magnetic, and electronic attributes, which are a result pf their unique incompletely filled 4f electronic orbitals and the vacant 5d electronic orbitals [9][10][11][12]. Conversely, molybdates hold considerable importance due to their remarkable mechanical strength, swift oxide ion conductivity, and advantageous structural, thermal, and chemical stabilities. These properties make them highly suitable for a range of applications, including laser photonics, optical signaling, photoluminescence, scintillators, and microwave technologies [13]. The low symmetric arrangement of rare earth (RE) cations within molybdates is a crucial factor in the development of effective materials. Recently, RE molybdates (RExMoyOz, where RE includes La, Ce, Nd, Pr, Sm, Dy, and Gd, among others) have garnered significant attention due to their diverse applications. These applications encompass catalysis, fuel cells, catalysts for CO and methane oxidation, as well as luminescent materials and phosphors, all attributed to their unique structural features and distinctive properties, such as atypical thermal expansion behaviour, rapid oxide-ion conduction, and notable catalytic and luminescent capabilities [14][15]. Dysprosium molybdate (DyxMoyOz, DyM) stands out among the different RE molybdates due to its unique physiochemical characteristics, including ferroelectricity, non-liner optical behaviour, and ferroelasticity. The notable electro-optic effect exhibited by Dy2(MoO4)3 presents significant potential for various device applications, indicating substantial technical promise[16][17].

The work uses DYM as electrode matrix, for the development of electrochemical sensors. The major objective of this work is to develop highly sensitive electrochemical sensor for the detection of CAP. In this work, we have successfully synthesized the Dym nanoparticles by a simple coprecipitation method. Synthesised nanomaterial is characterized using techniques such as X-ray diffraction (XRD) and Transmission electron microscopy. In addition to this, electrochemical techniques such as Cyclic Voltammetry (CV) and Electrochemical Impedance Spectroscopy (EIS) are also employed. Further the synthesized nanomaterial was fabricated on the pencil graphite electrode and was examined for the electrocatalytic property towards the detection of CAP.

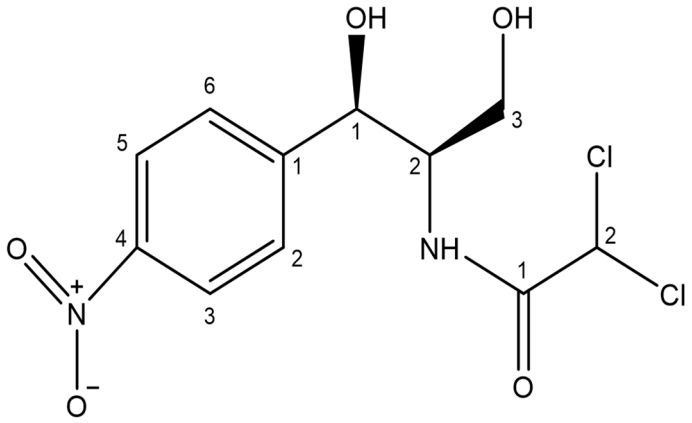

Fig 1: Structure of chloramphenicol

II. Experimental section

A. Chemicals and reagents.

Chloramphenicol was purchased from Sigma-Aldrich, Mumbai, India. Sodium molybdate (Na2MoO4), Dysprosium Nitrate (DyNO3)3, sodium hydrogen phosphate (Na2HPO4), sodium dihydrogen phosphate (NaH2PO4), Potassium chloride (KCl) are procured from Sigma-Aldrich, Mumbai, India, and SRL Pvt. Ltd., Mumbai, India. Throughout the experiment, double-distilled water was used, while all other materials and solvents used in this work were of analytical grade. XRD benchtop powder diffractometer, Proto Manufacturing Inc. (Canada), is used to record crystallographic information using Cu K Alpha radiation as a source (λ = 0.15443 nm). Morphological investigation of (DYM) and PGE is carried out using a FETEM, JSM-7100F (JEOL, Singapore), CV, EIS and differential pulse voltammetry (DPV) were performed using Biologic Science Instrument (SP-150, France). Hydrochloric acid (Hcl), Sodium hydroxide (NaOH), and Urea are purchased from SD Finer Chemicals, Mumbai, India.

B. Instruments

The structural crystallinity of the synthesized material was assessed using X-ray diffraction (XRD). The structural morphology and elemental composition of DYM were examined using HRTEM. All electrochemical measurements were conducted using a VersaSTAT-3.

C. Synthesis of DYM

Dysprosium molybdate was synthesized by a simple co-precipitation method. Briefly, 35 ml of 0.2 M (Na2MoO4) (1.69 g) and 35 ml of 0.1 M (DyNO3)3 (1.53g) were prepared using distilled water and were mixed in a 1:1 ratio to yield a homogeneous mixture. Subsequently, 5g of urea in 10ml water solution was added dropwise to the homogeneous solution. The resultant precipitate, obtained, washed with deionized water, and dried in a hot air oven. Finally, the solid product was heated in a muffle furnace at 650 °C for 5 h and was used for further experimental studies.

D. Analytical procedure

Fabrication of DYM onto the Pencil graphite electrode (Gr)

PGE was used for the fabrication of the working electrode. The electrode surface was polished using a PK-3 electrode polishing kit (0.05 mm aqueous polishing alumina and 1 mm polishing diamond) until a shining mirror surface was obtained and finally sonicated several times to remove loosely bound particles and later rinsed with milli-Q water and dried under nitrogen gas. The cleaned graphite rod was modified by drop-casting 6 µL of a homogeneous mixture. The modified electrode surface was dried at room temperature for 30 min and later washed with deionized water in order to remove any loosely bound particles from the electrode surface. The fabricated DyM sensor was stored at 4 °C until it was used for further studies.

Fig 2: Schematic representation of fabrication of DYM onto the pencil graphite electrode.

III. Results and Discussion

A. Characterizations

TEM Analysis

TEM analysis provides detailed structural information, and the results of the synthesized nanomaterial dysprosium molybdate are presented in Fig. 3. The low and high magnification TEM images are represented in A and B, which show HRTEM images of Dysprosium molybdate nanoparticles. Image A reveals aggregated,

irregularly shaped particles, while image B displays enlarged crystallites with well-defined lattice fringes, indicating a high degree of crystallinity.

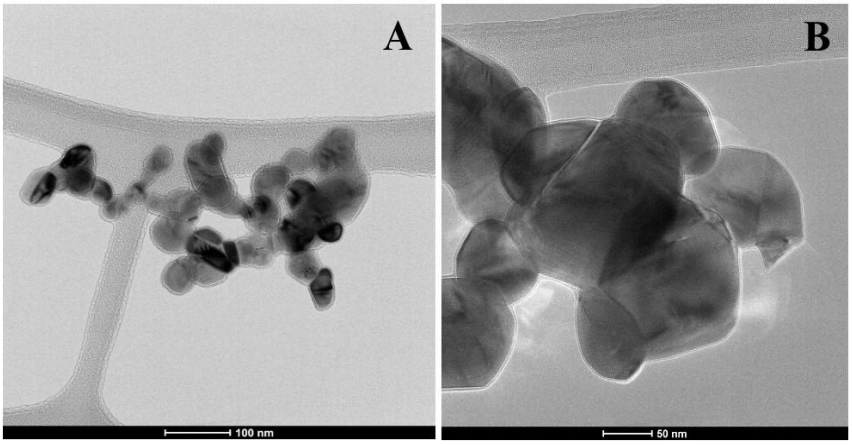

Fig 3: (A) HR TEM image of DyM with low magnification and (B) shows the TEM image of DyM with high magnification.

XRD Analysis

To evaluate the crystalline properties of the material, XRD analysis was carried out. XRD results portrayed the distinctive diffraction peaks at 2θ = 28.7, 31.5, 34.5, 39.9, 47.1, 49.9, 54.1, 58.6, and 59.90 were corresponded to the hkl planes of monoclinic Dy2MoO6, respectively. The formation and phase purity of monoclinic Dy2MoO6 were confirmed by matching it with previous XRD data[18]. The results obtained are in correlation with the previous results.

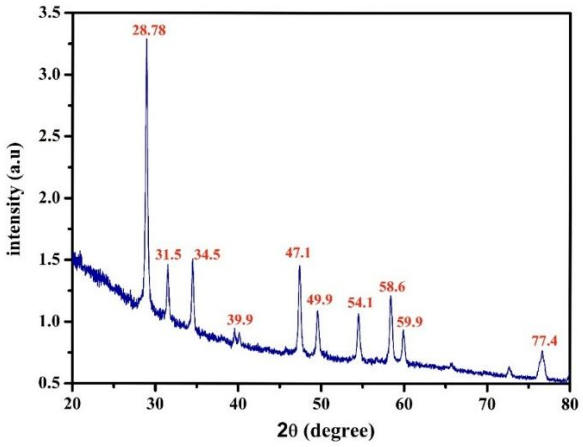

Fig 3: X-Ray diffraction pattern of DYM.

B. Electrochemical Studies

Electrochemical impedance spectroscopy (EIS)

To evaluate the electron transfer behaviour of the modified electrodes, EIS experiment was carried out for bare PGE, PGE/DYM electrodes, using 5 mM of [Fe (CN)6] 3-/4-solution containing 0.1 M KCl with an applied frequency ranging from 0.1 Hz to 100 kHz. The obtained results are represented in the form of Nyquist plots, as shown in Fig. 4. The results of EIS studies indicate that the charge transfer resistance (Rct) of the PGE electrode Rct 72.81 Ω is much higher than that of the PGE/DyM electrode indicating the poor electron conducting behaviour of the bare PGE compared to the latter. In contrast, a decreased Rct value for PGE/DyM Rct 45.83 Ω can be observed which may be attributed to the increased surface area of the modified electrode. Comparatively, the proposed PGE/DyM electrode showed a drastic decrease in Rct 26.98 Ω value indicating an enhanced surface coverage area and conductivity nature of the nanocomposite i.e., PGE/DyM composite. These results indicate the successful adhesion of nanomaterials onto the PGE and superior electron-conducting properties of the proposed electrode.

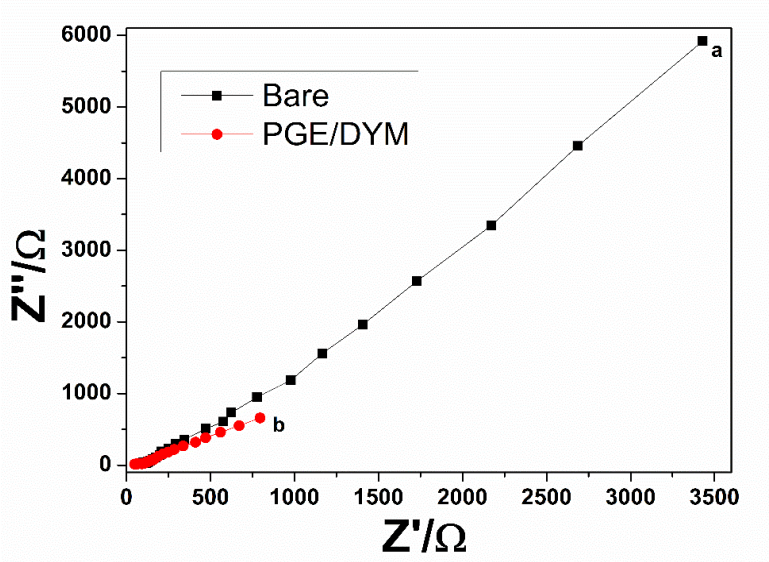

Fig 4: (A) EIS curve of (a) bare PGE (b) PGE/DYM using 5 mM [Fe (CN)6] 3-/4− containing 0.1 M KCl solution.

C. Effect of pH

The influence of pH on the oxidation peak current and peak potential of PGE/DYM electrode was scrutinized by monitoring DPVs using 10 mM CAP at different pH values in the range of 3.5–9.5 at a scan rate of 50 mV/s. As can be seen in Fig. 5 the peak current increased with rising pH values, illustrating the proton transfer process on the surface of PGE/DYM towards CAP. In addition, the peak current of CAP increased gradually and then decreased with an optimum peak current at pH 7.5. Thus, pH 7.5 was chosen for further studies.

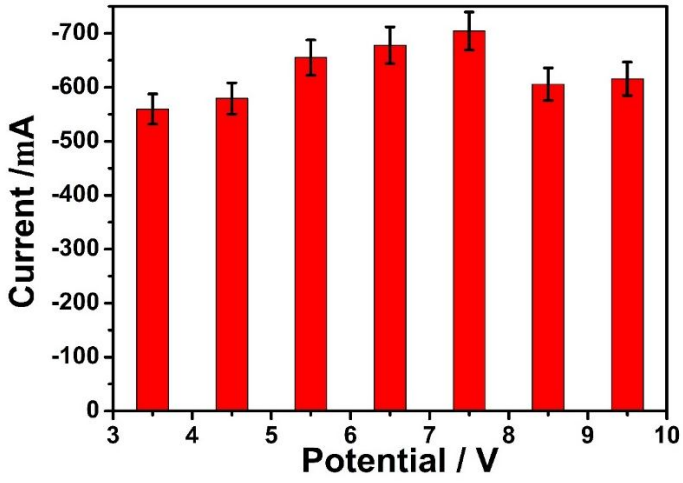

Fig. 5: Effect of pH (3.5–9.5) on PGE/DYM modified electrode in N2 saturated PBS solution in presence of 10 mM CAP.

D. Effect of Scan Rate

The effect of the scan rate on the modified PGE/DYM is studied using CV. Fig 6 A shows the cyclic voltammogram of the PGE/DYM for different scan rates such as 25, 50, 75, 100, 125, up to 275 mV s-1 (a-k) in the presence of 10 mM CAP. The CV results show an enhancement in redox peak currents with an increase in scan rate. Furthermore, the cathodic and anodic peak currents show a good linear relationship with the scan rate (Fig. 6 B and C). The calculated regression coefficients for scan rate cathodic and anodic current responses are R_2 =99.12 and R_2 = 99.60, respectively. The calculated regression coefficients for the square root of scan rate cathodic and anodic current responses are R_2 = 99.34 and R_2 = 98.68. This is attributed to the larger surface area contributing to faster electron transferability. The value of the regression coefficients R_2 is close to 1.0 suggesting that the overall electrochemical reaction at the PGE/DYM electrode is adsorption-controlled.

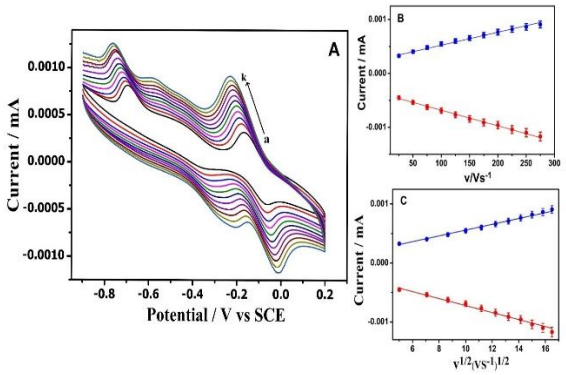

Fig. 6: (A) CVs of PGE/CAP in 0.1 M PBS (pH 7.5) containing 10 mM CAP at different scan rates. (B) Peak current Vs. Scan rate, (C) Peak current Vs. square root of scan rate.

E. Electrochemical Determination of CAP

The electrochemical performance of the PGE/DYM electrode is investigated by measuring CV response for different concentration of CAP. Fig. 7 A shows CV obtained for PGE/DyM in the presence of different concentrations of CAP (10- 50 mM) in nitrogen saturated PBS (pH 7.5) at a scan rate of 50 mV s-1. A good oxidation and reduction peak currents are observed in the presence of CAP. The increase in CAP concentration resulted in enhanced reduction current that is ascribed to the oxidation of CAP at the PGE/DyM (Scheme 1). The anodic peak current increased linearly from 10 to 50 mM of CAP with a correlation coefficient (R2) of 0.9752. This signifies the reliability of the sensor performance for applications.

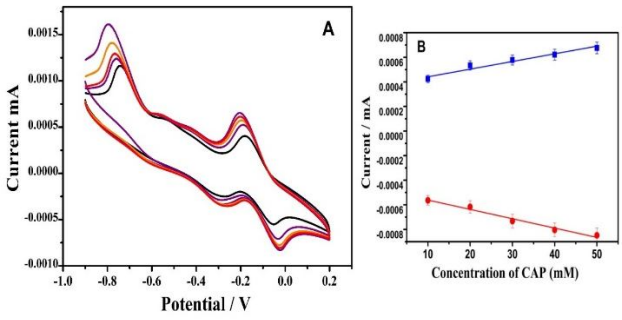

Fig. 7: A CVs of PGE/DYM electrode at different CAP concentrations (10 to 50 mM) in 0.1M PBS (pH7.5). (B) Calibration plot of current vs. CAP concentration.

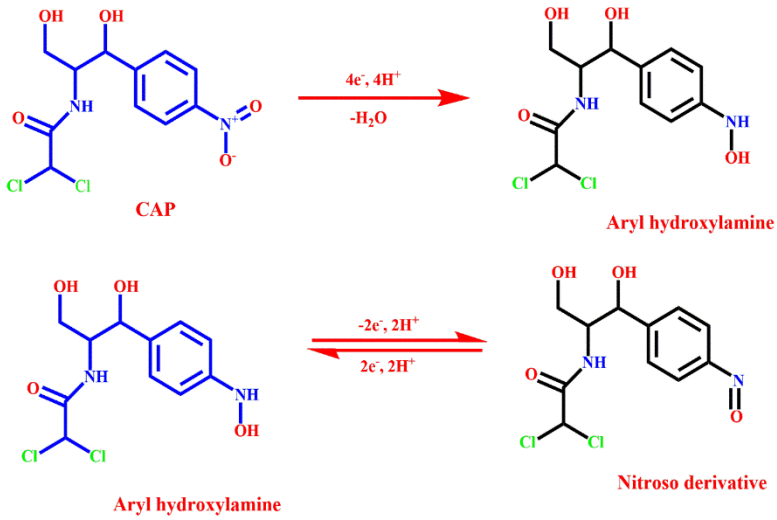

Figure 8. Scheme 1: Electrochemical reduction process of CAP.

Further, DPV experiments are performed to calibrate the sensor for lower concentrations of CAP. DPV is run with 0.1 PBS solution in the potential range -0.6 to 0.6 V. Fig. 8 shows the DPV current response at lower concentrations from 100 to 1000 µM of CAP. A linear relationship is obtained between the CAP concentration and current signal for PGE/DyM this linear relation has a correlation coefficient of R2 = 0.982. With this data, the critical parameters of the sensor, i.e, limit of detection (LOD), sensitivity, and quantification limit (LOQ) are calculated using the following equations (Equations 1, 2, and 3, respectively).

$$LOD = \frac{3\sigma}{s} \quad \text{Eq 1}$$

$$sensitivity = \frac{s}{surface\ area\ of\ electrode} \quad \text{Eq 2}$$

$$LOQ = \frac{10\sigma}{s} \quad \text{Eq 3}$$

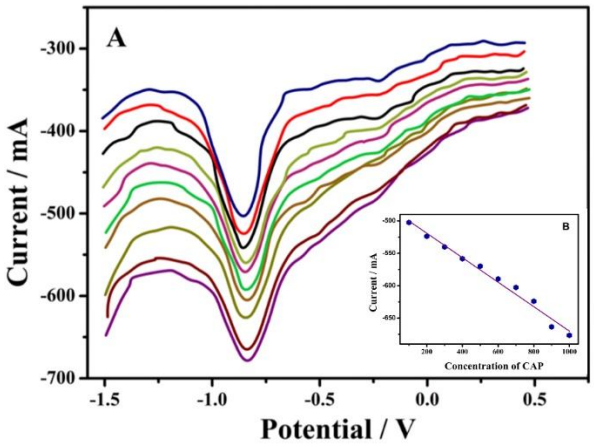

Fig. 8: A. DPVs of the PGE/DYM electrode in the presence of varying CAP concentration (100 to 1000 µM) in 0.1 M PBS solution. B. Calibration plot of peak current versus CAP concentration

Here, σ is the standard deviation of the blank, and S is the slope of the calibration plot (Fig. 8 B). The sensitivity, LOQ, linear range, and LOD determined using experimental data are 18.87 µA $mM^{-1}cm^{-2}$, 2.496 µM, 100 – 1000 µM, and 0.7488 µM, respectively. These values are fairly comparable with CAP sensors reported (Table 1), which marks the as-developed sensor as a promising candidate.

TABLE I

Matrix	Linear Range (µM)	LOD (µM)	Reference
MWCNT	1.0 - 1.0	1.0	[19]
MMB	0.050-1.0	44	[20]
MIP	10-100	3.0-1.0	[21]
CZE	100-900	0.99	[22]
DyM	100-1000	0.748	Present work

F. Stability, repeatability and reproducibility

These experiments are very crucial to comment on the sensor's practical applicability and reliability. The stability, reproducibility, and repeatability were analysed at PGE/DyM using CV technique in 0.1 M PBS having pH 7.5 containing 0.1 mM CAP with the scan rate of 0.1 V/s. The excellent stability of the PGE/DyM was examined by running 30 successive CV cycles and observed 96.47 % retention in current response.

The repeatability of the sensor is confirmed by measuring the CV response for 10 µM CAP in 0.1M PBS solution for twenty electro-analytical cycles in the potential range of −0.2 to +0.6 V at a scan rate 50 mV s-1.

The % of degradation was evaluated by using the formula

$$\text{Percentage degradation} = \frac{I_{pn}}{I_{p1}} \times 100$$

Here, I_{pn} is the oxidation peak current of the last cycle, and I_{p1} is the anodic peak current of the first cycle; the value of percentage degradation was found to be 3.53%. This shows the exceptional stability of the proposed sensor. The reproducibility of the sensor was studied for CAP at 5 parallelly modified electrodes, and observed

good reproducible response was observed with a relative standard deviation (RSD) of 3.25 %. While repeatability of PGE/DyM was performed for CAP detection with unchanged electrode with RSD 2.65 %. These results demonstrates that the proposed PGE/DyM has impressive stability, reproducibility and repeatability.

IV. Conclusions

In this study, DyM nanoparticles were successfully synthesised via a simple co-precipitation method and employed as an efficient electrochemical sensing material for the detection of CAP. The structural and morphological analyses confirmed the formation of crystalline monoclinic Dy2MoO6 with well-defined nanostructures. Electrochemical studies demonstrated that the PGE/DyM-modified electrode exhibited excellent electrocatalytic activity towards CAP with high sensitivity, low detection limit (0.7488 µM), and a wide linear range (100-1000 µM). the developed sensor also showed good reproducibility, repeatability, and operational stability, indicating its potential for practical applications in pharmaceutical and environmental monitoring. These findings suggest that DyM-based sensors could serve as promising platforms for the cost-effective and sensitive detection of CAP and possibly other antibiotic residues.

References

[1] L. Fu et al., "Graphene-based electrochemical sensors for antibiotic detection in water, food and soil: A scientometric analysis in CiteSpace (2011–2021)," Chemosphere, vol. 297, p. 134127, 2022, doi: https://doi.org/10.1016/j.chemosphere.2022.134127.

[2] S. B. Ravikumar et al., "Cadmium-doped titanium dioxide material for electrochemical sensing of chloramphenicol in diverse real-world samples: a DFT analysis," Ionics (Kiel)., vol. 30, no. 12, pp. 8591–8604, 2024.

[3] G. Yang and F. Zhao, "Electrochemical sensor for chloramphenicol based on novel multiwalled carbon nanotubes@molecularly imprinted polymer," Biosens. Bioelectron., vol. 64, pp. 416–422, 2015, doi: https://doi.org/10.1016/j.bios.2014.09.041.

[4] K. Kaewnu, K. Promsuwan, P. Kanatharana, P. Thavarungkul, and W. Limbut, "A Simple and Sensitive Electrochemical Sensor for Chloramphenicol Detection in Pharmaceutical Samples," J. Electrochem. Soc., vol. 167, no. 8, p. 87506, 2020, doi: 10.1149/1945-7111/ab8ce5.

[5] S. Subbareddy et al., "Synergistic innovation: MOF@GCN hybrid for electrochemical detection of flutamide—bridging experimental, computational, and real-world applications," Microchim. Acta, vol. 192, Apr. 2025, doi: 10.1007/s00604-025-07164-3.

[6] A. S. Santhosh et al., "Synthesis and application of a 0D/2D nanocomposite for the nanomolar level detection of an antiandrogen drug," New J. Chem., 2022, doi: 10.1039/D2NJ01967A.

[7] V. Vinothkumar, M. Abinaya, and S.-M. Chen, "Ultrasonic assisted preparation of CoMoO4 nanoparticles modified electrochemical sensor for chloramphenicol determination," J. Solid State Chem., vol. 302, p. 122392, 2021, doi: https://doi.org/10.1016/j.jssc.2021.122392.

[8] H. Chen, J. Hu, G.-D. Li, Q. Gao, C. Wei, and X. Zou, "Porous Ga–In Bimetallic Oxide Nanofibers with Controllable Structures for Ultrasensitive and Selective Detection of Formaldehyde," ACS Appl. Mater. Interfaces, vol. 9, no. 5, pp. 4692–4700, Feb. 2017, doi: 10.1021/acsami.6b13520.

[9] A. P. Alivisatos, "Semiconductor clusters, nanocrystals, and quantum dots," Science (80-.)., vol. 271, no. 5251, pp. 933–937, 1996.

[10] M. Rahimi-Nasrabadi, F. Ahmadi, and A. Fosooni, "Influence of capping agents additives on morphology of CeVO 4 nanoparticles and study of their photocatalytic properties," J. Mater. Sci. Mater. Electron., vol. 28, pp. 537–542, 2017.

[11] M. Rahimi-Nasrabadi, S. M. Pourmortazavi, M. R. Ganjali, P. Novrouzi, F. Faridbod, and M. S. Karimi, "Preparation of dysprosium carbonate and dysprosium oxide efficient photocatalyst nanoparticles through direct carbonation and precursor thermal decomposition," J. Mater. Sci. Mater. Electron., vol. 28, pp. 3325–3336, 2017.

[12] F. Ahmadi, M. Rahimi-Nasrabadi, and M. Behpour, "Synthesis Nd 2 TiO 5 nanoparticles with different morphologies by novel approach and its photocatalyst application," J. Mater. Sci. Mater. Electron., vol. 28, pp. 1531–1536, 2017.

[13] J. V. B. Moura et al., "Synthesis, characterizations, and antibacterial properties of PbMoO4 nanocrystals," Arab. J. Chem., vol. 11, no. 6, pp. 739–746, 2018.

[14] M.-K. Xu, Z.-H. Ouyang, and Z.-R. Shen, "Topological evolution of cerium (III) molybdate microflake assemblies induced by amino acids," Chinese Chem. Lett., vol. 27, no. 5, pp. 673–677, 2016.

[15] R. Karthik, J. Vinoth Kumar, S.-M. Chen, C. Karuppiah, Y.-H. Cheng, and V. Muthuraj, "A study of electrocatalytic and photocatalytic activity of cerium molybdate nanocubes decorated graphene oxide for the sensing and degradation of antibiotic drug chloramphenicol," ACS Appl. Mater. Interfaces, vol. 9, no. 7, pp. 6547–6559, 2017.

[16] M. Zhong et al., "Crystalline phase distribution of Dy2 (MoO4) 3 in glass induced by 250 kHz femtosecond laser irradiation," Opt. Mater. Express, vol. 2, no. 8, pp. 1156–1164, 2012.

[17] M. Roy, R. N. P. Choudhary, and H. N. Acharya, "X-ray and thermal studies of ferroelectric Dy 2 (MoO 4) 3," J. Therm. Anal., vol. 35, pp. 1471–1476, 1989.

[18] J. A. Alonso, F. Rivillas, M. J. Martínez-Lope, and V. Pomjakushin, “Preparation and structural study from neutron diffraction data of R2MoO6 (R=Dy, Ho, Er, Tm, Yb, Y),” J. Solid State Chem., vol. 177, no. 7, pp. 2470–2476, 2004, doi: https://doi.org/10.1016/j.jssc.2004.03.046.
[19] M. R. Ganjali, T. Alizade, and P. Norouzi, “Chloramphenicol biomimetic molecular imprinted polymer used as a sensing element in nano-composite carbon paste potentiometric sensor,” Int. J. Electrochem. Sci., vol. 7, no. 5, pp. 4800–4810, 2012.
[20] L. Codognoto, E. Winter, K. M. Doretto, G. B. Monteiro, and S. Rath, “Electroanalytical performance of self-assembled monolayer gold electrode for chloramphenicol determination,” Microchim. Acta, vol. 169, pp. 345–351, 2010.
[21] M. L. Mena, L. Agüí, P. Martinez-Ruiz, P. Yanez-Sedeno, A. J. Reviejo, and J. M. Pingarrón, “Molecularly imprinted polymers for on-line clean up and preconcentration of chloramphenicol prior to its voltammetric determination,” Anal. Bioanal. Chem., vol. 376, pp. 18–25, 2003.
[22] A. Wang, L. Zhang, and Y. Fang, “Determination and separation of chloramphenicol and its hydrolysate in eye-drops by capillary zone electrophoresis with amperometric detection,” Anal. Chim. Acta, vol. 394, no. 2–3, pp. 309–316, 1999.